Algal Research 23 (2017) 66–77

Contents lists available at ScienceDirect

Algal Research

journal homepage: www.elsevier.com/locate/algal

Effects of chrysolaminarin synthase knockdown in the diatom *Thalassiosira pseudonana*: Implications of reduced carbohydrate storage relative to green algae

Mark Hildebrand *, Kalpana Manandhar-Shrestha, Raffaela Abbriano

Marine Biology Research Division, Scripps Institution of Oceanography, UC San Diego, La Jolla, CA, United States

ARTICLE INFO

Article history:
Received 19 September 2016
Received in revised form 14 December 2016
Accepted 24 January 2017
Available online 29 January 2017

Keywords:
Diatom
Chrysolaminarin
Carbon flux
Storage carbohydrate
Productivity

ABSTRACT

In all organisms, the flux of carbon through the fundamental pathways of glycolysis, gluconeogenesis and the pyruvate hub is a core process related to growth and productivity. In unicellular microalgae, the complexity and intracellular location of specific steps of these pathways can vary substantially. In addition, the location and chemical nature of storage carbohydrate can be substantially different. The role of starch storage in green algae has been investigated, but thus far, only a minimal understanding of the role of carbohydrate storage in diatoms as the β-1,3-glucan chrysolaminarin has been achieved. In this report, we aimed to determine the effect of specifically reducing the ability of *Thalassiosira pseudonana* cells to accumulate chrysolaminarin by knocking down transcript levels of the chrysolaminarin synthase gene. We monitored changes in chrysolaminarin and triacylglycerol (TAG) levels during growth and silicon starvation. Transcript-level changes in genes encoding steps in chrysolaminarin metabolism, and cytoplasmic and chloroplast glycolysis/gluconeogenesis, were monitored during silicon limitation, highlighting the carbon flux processes involved. We demonstrate that knockdown lines accumulate less chrysolaminarin and have a transiently increased TAG level, with minimal detriment to growth. The results provide insight into the role of chrysolaminarin storage in diatoms, and further discussion highlights differences between diatoms and green algae in carbohydrate storage processes and the effect of reducing carbohydrate stores on growth and productivity.

1. Introduction

During the course of evolutionary history, unicellular microalgae have utilized different carbohydrates as energy and carbon storage molecules, and altered the location of storage of carbohydrates in the cell, resulting in dramatic differences in storage forms and locations [1–3]. Carbohydrate stores range from insoluble starch, hydrosoluble glycogen, and water soluble β-1,3-glucans such as chrysolaminarin. The location of carbohydrate stores include: inside the chloroplast, (particularly around the pyrenoid), in the cytoplasm, in vesicles surrounding the chloroplast endoplasmic reticulum (ER), within the periplastid compartment (which is between the outer chloroplast membrane and periplastid membrane in secondary endosymbionts) and in a cytoplasmically-localized vacuole [3].

One might suppose that a fundamental cellular feature such as the type and location of carbohydrate storage would have an optimum arrangement, and such an arrangement would have been "settled on" at some early stage in evolution. Because this is not the case, it is likely that over time, different selective pressures for efficient carbohydrate storage and utilization have been applied, resulting in different "solutions" for which type of carbohydrate was utilized and where it was stored. Environmental conditions have varied throughout evolutionary history, with substantial changes in atmospheric temperature, O_2 and CO_2 levels (for long time periods CO_2 was 5–12-fold higher than currently – [4]), and geological changes have affected the average depth and extent of mixing of the oceans, which altered light and nutrient regimes [5–7]. The requirement for efficient growth is a major selective pressure on microalgae, and since intracellular carbon flux is the process by which cellular energy and molecular components needed for growth are derived, changes in carbon storage location and type might be expected to occur. It is not likely that all extant intracellular arrangements are optimal under current environmental conditions, but is it likely that they work well enough to enable the organism to compete successfully, albeit for some organisms in certain niches. Differences in carbohydrate type and storage could affect a variety of aspects of cellular function, including photosynthetic efficiency, carbon fixation, carbon flux and partitioning, carbohydrate storage, lipid accumulation, cellular energetics and cross-compartmental interactions. They also could influence what time of day or night is optimal for cell division. Investigating carbon flux processes in evolutionarily-diverse classes of microalgae

* Corresponding author.
E-mail address: mhildebrand@ucsd.edu (M. Hildebrand).

http://dx.doi.org/10.1016/j.algal.2017.01.010

could lead to a better understanding of the relative advantages and drawbacks to particular organizational schemes, which will inform aspects of productivity and ecological success, as well as define a wider variety of options for synthetic biology approaches. Understanding how to manipulate particular schemes could improve productivity for algal biotechnological applications.

In stramenopiles, such as diatoms, carbohydrate is stored as a soluble β-1,3-linked glucan called chrysolaminarin in a large cytoplasmically-localized chrysolaminarin vacuole [8–10]. Water soluble storage carbohydrates are more accessible energetically and biophysically than insoluble starch [8,15], and such differences should affect intracellular energetics and carbon flux. Chrysolaminarin contents

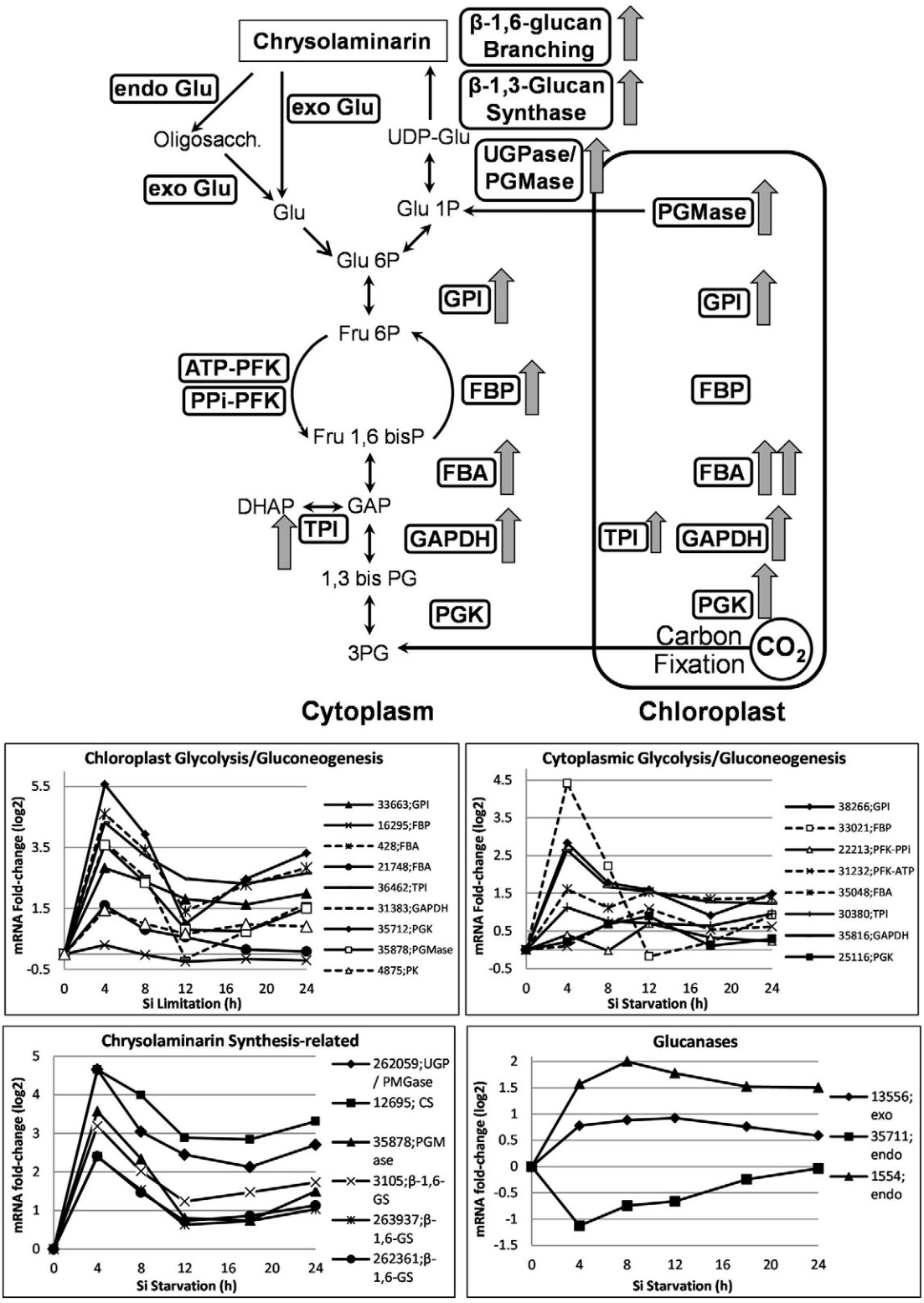

Fig. 1. mRNA-level response during silicon starvation of genes involved in chrysolaminarin synthesis and breakdown, and cytoplasmic and chloroplast glycolysis/gluconeogenesis. Top) Pathways and enzymes involved in the analysis. Enzymes are bolded and boxed. Arrows identify enzymes whose mRNAs are induced at least 2-fold at 4 h. Bottom) plots of mRNA fold changes relative to 0 h of silicon starvation. Genes are identified by their protein ID number, Thaps vers. 3.

of 12–33% DW have been documented in different diatom species under particular conditions [11,12], and under certain conditions, up to 80% of total cellular carbon has been documented as chrysolaminarin [14]. Measurements indicate that dynamic changes in cellular chrysolaminarin content occur; for example, in *Odontella aurita*, chrysolaminarin content varied under different culture conditions from 15 to 61% of DW [13].

When diatoms are limited for silicon or nitrogen, growth arrest results in higher accumulation of storage carbon as carbohydrate and lipid [16–19]. Thus, nutrient limitation provides conditions to examine the induction of processes involved in carbon storage. Roessler [20,21] examined the response of chrysolaminarin and triacylglycerol (TAG) synthesis enzymes in response to silicon limitation in *Cyclotella cryptica*. Fig. 1 depicts steps involved in chrysolaminarin metabolism. After 4 h in silicon-free medium, UGPase enzymatic activity did not change, beta-1,3-glucan (chrysolaminarin) synthase activity decreased 1.4-fold, and acetyl-CoA carboxylase (ACCase) activity increased nearly 2-fold [20]. ^{14}C-labeling experiments showed a shift in partitioning of label, with a decrease in labeling of chrysolaminarin and an increase with lipid [16]. Granum and coworkers [17,22] performed a series of experiments investigating glucan metabolism on nitrogen-limited *Skeletonema costatum*. ^{14}C pulse-labeling indicated that 85% of label was incorporated into β-1,3-glucan within 4 h of nitrogen limitation [17], suggesting initial rapid storage of fixed carbon into carbohydrate. Chase experiments performed by adding ammonium revealed labeling of free amino acids, indicating mobilization of the chrysolaminarin reserves into biosynthetic processes. During the course of nitrogen limitation over several days, β-1,3-glucan levels increased 1.6–2.3 fold [22]. In exponentially growing non-limited cultures on a day:night cycle, β-1,3-glucan levels varied between 17 and 42% of cellular organic carbon at the beginning and end of the light period, respectively. Overall, these studies suggest a light dependence on chrysolaminarin levels, and a preference for initial storage of fixed carbon as chrysolaminarin, followed by mobilization of that carbon into biosynthesis of compounds such as lipids and amino acids. Growth cessation increases chrysolaminarin levels.

Initial research into the enzymology of chrysolaminarin synthesis in *C. cryptica* involved an attempt to clone the UGPase gene by PCR and subsequent screening of a genomic DNA library [23]. Sequencing revealed a single ORF with both UGPase and phosphoglyceromutase (PGMase) domains. The latter catalyzes the conversion of G-6-P to G-1-P; thus sequential steps in processing precursors for chrysolaminarin synthesis were encoded on the same polypeptide. A candidate for the β-1,3-glucan synthase gene was identified by homology searches of diatom genome sequences [24], and because only one gene was identified in each genome, it is likely to be the chrysolaminarin synthase. The chrysolaminarin structure includes β-1,6 branching, and two genes encoding enzymes likely involved in that process were recently characterized by complementation of yeast mutants [25]. Enzymes encoded by these genes were shown to be vacuolarly targeted in the diatom [25], consistent with their proposed function.

Recent work has knocked down or knocked out the UGPase/PGMase gene in the diatom *Phaeodactylum tricornutum* [26,27]. In both studies, the authors did not mention the dual functionality of the gene (UGPase/PGMase); and perhaps assumed it encoded only an UGPase. Both RNAi and antisense approaches were applied to knock down the UGPase/PGMase gene, and substantial decreases in chrysolaminarin occurred with either approach [26]. A consequence of reducing carbohydrate stores could be repartitioning of carbon to other forms, particularly fatty acids (FAs) or TAG as a longer term carbon store. The best knockdown line accumulated 25% more FA than controls [26]. TAG was not specifically monitored, nor was nutrient limitation done to evaluate possible differences in maximal TAG yield. A slight decrease in growth rate was apparent with the knockdowns [26], suggesting some metabolic or energetic drain. In the study in which a knockout line was generated using a TALEN approach [27], the knockout line accumulated as much TAG in nutrient replete medium as wild-type cells did under nitrogen limitation, and nitrogen-limited knockouts accumulated about 3 times more TAG than nitrogen-limited wild-type. No data on the effect of knockdown on growth or chrysolaminarin content was reported [27].

Thus far, the involvement of the β-1,3-glucan (chrysolaminarin) synthase in carbon storage in diatoms has not been investigated. In this report, we aimed to determine the effect of specifically reducing the ability of *Thalassiosira pseudonana* cells to accumulate chrysolaminarin by knocking down transcript levels of the chrysolaminarin synthase gene. Changes in chrysolaminarin and TAG levels during growth and silicon starvation growth arrest were monitored, as well as transcript-level changes in genes involved in core carbon flux processes to generate these molecules. The results provide insight into the role of chrysolaminarin storage in diatoms, and highlights differences between diatoms and green algae in carbohydrate storage processes and the effect on growth and productivity of reducing carbohydrate stores.

2. Materials and methods

2.1. Algal strains and culture conditions

Axenic cultures of the marine diatom *Thalassiosira pseudonana* (CCMP 1335) were grown in artificial seawater (ASW) [28] at 18–20 °C under continuous illumination at 150 μmol m^{-2} s^{-1}. For silicon starvation, exponentially grown cultures were harvested and washed twice with silicon-free ASW and then incubated at 1.0×10^6 cells·ml^{-1} in silicon-free ASW in polycarbonate flasks. Culture density was determined either using a hemocytometer or a Muse® Cell Analyzer (Millipore Corp., Billerica MA, USA).

2.2. Sequence comparison analysis

Amino acid sequences for comparison (listed in Fig. 3) were selected from best BLAST hits and representative examples of beta-1,3-glucan synthase sequences from stramenopiles, green algae, vascular plants, and fungi. The tree was generated using CLC workbench 6 software.

2.3. Construction of expression vectors for knockdown of chrysolaminarin synthase

Antisense RNA expression was employed to knockdown transcripts for the chrysolaminarin synthase (Thaps3_12695). A reverse complementary sequence of a portion of the gene was amplified through PCR using genomic DNA of wild type *T. pseudonana* as the template with forward primer 5′-CGATGAAAACGGTGAAACAGCTG-3′ and reverse primer 5′-CATCGAGTCATTTGTATCTTGGAG-3′. The PCR product was cloned into a Gateway donor vector (pDONR 221 attB1-attB2) using BP Clonase (Life Technologies Corp., Carlsbad CA, USA) to create an entry clone. The expression vector was then generated by LR recombination of the entry vector and a destination vector. The expression vector thus contained the fucoxanthin chlorophyll *a*/c-binding gene (fcp) promoter, selective marker for nourseothricin (NAT) [29], anti-sense sequence, and fcp terminator.

2.4. Transformation procedure and characterization of transgenic lines

The antisense expression vector for Thaps3_12695 was used to transform *T. pseudonana* using the Bio-Rad biolistic particle delivery system. NAT-resistant transgenic cells were selected either in liquid culture or on agar plates containing 100 μg/ml nourseothricin (clonNAT, Werner BioAgents, Jena, Germany). Colonies were further screened by PCR analysis and DNA sequencing. For DNA extraction, 4–5 × 10^6 cells were harvested and washed once with sterilized water. The supernatant was discarded and 25 μl TE was added to the pellet. Cells were then

ruptured by 3 cycles of freezing on dry ice and thawing at 65 °C followed by heating at 95 °C for 5 min. Supernatants were collected after centrifugation at 12,000 rpm, and an aliquot used for PCR.

2.5. Soluble carbohydrate analysis

One hundred milliliter of either a 0.5 or 1.0×10^6 cells·ml^{-1} culture of *T. pseudonana* were harvested by filtration, washed in 0.45 M NaCl, pelleted in a microfuge, and the pellet was stored frozen at −20 °C. Samples were resuspended in 5 ml 0.05 M H_2SO_4, and incubated at 60 °C for 10 min. Samples were centrifuged at 4000 × *g* for 2 min, and 2 ml of supernatant was transferred to a new tube. Freshly made 3% phenol in water (0.5 ml) and 5 ml concentrated H_2SO_4 was added to the tube and the sample was incubated for 30 min at room temperature. Absorbance at 485 nm was measured and compared to a dilution series of glucose at known concentration.

2.6. Staining of neutral lipids using BODIPY

To analyze neutral lipid [30–32], 1.0–2.0 × 10^6 cells were harvested, pelleted, and re-suspended in in 0.45 M NaCl. Cells were stained with 2.6 μg·ml^{-1} BODIPY (4, 4-difluoro-3a, 4a diaza-s-indacene) (Invitrogen, Thermo Fisher Scientific, Carlsbad CA, USA) incubating for 15–20 min at room temperature in the dark.

2.7. Staining of algal cells using aniline blue

Cells were harvested by centrifugation and fixed with 1% glutaraldehyde to permeabilize the membrane. Cells were washed and resuspended in 0.1 M potassium phosphate buffer (pH 7.4) and then stained with 1 mg·ml^{-1} aniline blue (9) for 10 min.

2.8. Fluorescence microscopy

To observe chrysolaminarin, cells stained with aniline blue were visualized under the Zeiss Axio Observer.Z1 microscope with Plan-Apochromat 63x/1.40 Oil DIC M27 objective and filter set 21 HE FURA for aniline blue staining and 05 filter set (Ex 395–440 nm, FT 460 nm, Em 470 nm LP) for chlorophyll.

2.9. Imaging flow cytometer analysis of BODIPY and aniline blue staining

Quantification of BODIPY (as a proxy of TAG content) and aniline blue (for chrysolaminarin content) was done using an ImageStream X (Millipore Corp. Billerica MA, USA) imaging flow cytometer. Cells were excited with a 408-nm laser at 10 mW for aniline blue, and a 488-nm laser at 20 mW for BODIPY, and brightfield and fluorescent images were collected for 20,000 events. Data were collected at 40× magnification. Data was analyzed using Amnis IDEAS™ software. Data were collected on fluorescently stained and unstained cells, and unstained cells were used to define a gated population which represented background. Cells with higher fluorescence constituted the treatment population. Populations were further analyzed by selecting for in-focus, single cells, which enables accurate quantitation. The mean of the population was determined from the data and reported.

2.10. Fast repetition rate fluorometry

Fast repetition rate fluorescence (FRRF) (Chelsea Instruments, West Molesey, UK) was used to estimate photosynthetic quantum yields and photosynthetic rates. We measured maximum quantum efficiency of photochemistry of *Psi*I (Fv/Fm) in the wild type and transgenic knockdown cultures. Exponentially grown and silicon starved wild type and transgenic cells were placed in a dark chamber for 10 mins and Fv/Fm were measured according to the manufacturer's instruction.

3. Results

3.1. Characterization of genes involved in chrysolaminarin metabolism

Based on sequence homology searches, the *T. pseudonana* genome contained two genes potentially involved in synthesis of immediate precursors for β-1,3-linked glucan, and another gene responsible for β-1,3-glucan synthesis itself. These included a PGMase (Thaps3_35878), which was predicted to be chloroplast-targeted, a protein with both PGMase and UGPase domains (Thaps3_262059) corresponding to the enzyme characterized by Roessler [23], with no predicted organellar targeting, and a β-1,3-glucan synthase (Thaps3_12695), which we will henceforth call the chrysolaminarin synthase, with no clearly predicted organellar targeting. The presence of the predicted chloroplast targeted PGMase and cytoplasmic PGMase/UGPase indicates that glucose-1-phosphate can be generated in either compartment (Fig. 1). In addition, three genes (Thaps3_3105, 262361, and 263937) involved in generating β-1,6 linkages as are found in chrysolaminarin were identified, as reported in Huang et al. [25], these correspond to TSG1, TSG2, and TSG3 respectively in *P. tricornutum*. Thaps3_263937 had predicted ER targeting, and Thaps3_3105 and 262361 had predicted periplastid targeting due to a reasonable ChloroP [33] score, however their homologs have been directly localized to the vacuolar membrane in *P. tricornutum* [25]. Periplastid targeting predictions are not very robust in diatoms [34], which may explain the discrepancy.

Examination of the chrysolaminarin synthase gene sequence revealed three groups of predicted transmembrane regions (Fig. 2), as well as FKS and β-1,3-glucan synthase domains. From the amino towards the carboxyl terminus, the transmembrane regions consist of 7, 5–7, and 8–10 predicted individual transmembrane spanning segments (Fig. 2). Comparison with the *S. cerevisiae* β-1,3-glucan synthase indicates that the diatom protein has an additional set of transmembrane segments near the amino-terminus (Fig. 2). This portion of the sequence has no homologs, therefore its function is unknown. The FKS and β-1,3-glucan synthase domains are typical of fungal glucan synthases [35]. Multiple protein alignment is consistent with the diatom chrysolaminarin synthases being similar to fungal β-1,3-glucan synthases, which are distinct from those in plants and green algae (Fig. 3).

All three β-1,6-glucan branching enzymes have KRE6 and SKN1 domains (data not shown and [26]), which are characteristic of yeast enzymes [36]. Interestingly, all three enzymes also encode a laminin G domain, which are usually found in Ca^{2+}-mediated receptors [37]. The function of this domain in an intracellular vacuole is unclear. The fused PGMase/UGPase has homologs in stramenopiles, but BLAST searching identified homologs to only the PGMase domain in plants (data not shown), suggesting a gain in function through gene fusion during evolutionary history.

3.2. Transcript-level changes of genes involved in chrysolaminarin metabolism and chloroplast and cytoplasmic glycolysis

We mined a whole genome microarray dataset [19] to evaluate transcript-level changes of genes involved in chrysolaminarin synthesis and breakdown and cytoplasmic and chloroplast glycolysis/gluconeogenesis after a *T. pseudonana* culture was silicon starved (Fig. 1). Transcripts for genes involved in the immediate precursor and chrysolaminarin synthase and branching steps were all highly upregulated by 4 h post silicon starvation (Fig.1, Table S1). Most cytoplasmic and chloroplast glycolysis/gluconeogenesis gene transcripts were significantly upregulated (greater than 2-fold). The data indicated upregulation in the direction of gluconeogenesis in both compartments (Fig. 1, Table S1), consistent with the flux of carbon towards chrysolaminarin synthesis. Direct measurement of changes in soluble carbohydrate (chrysolaminarin) levels upon transition of cells into silicon free

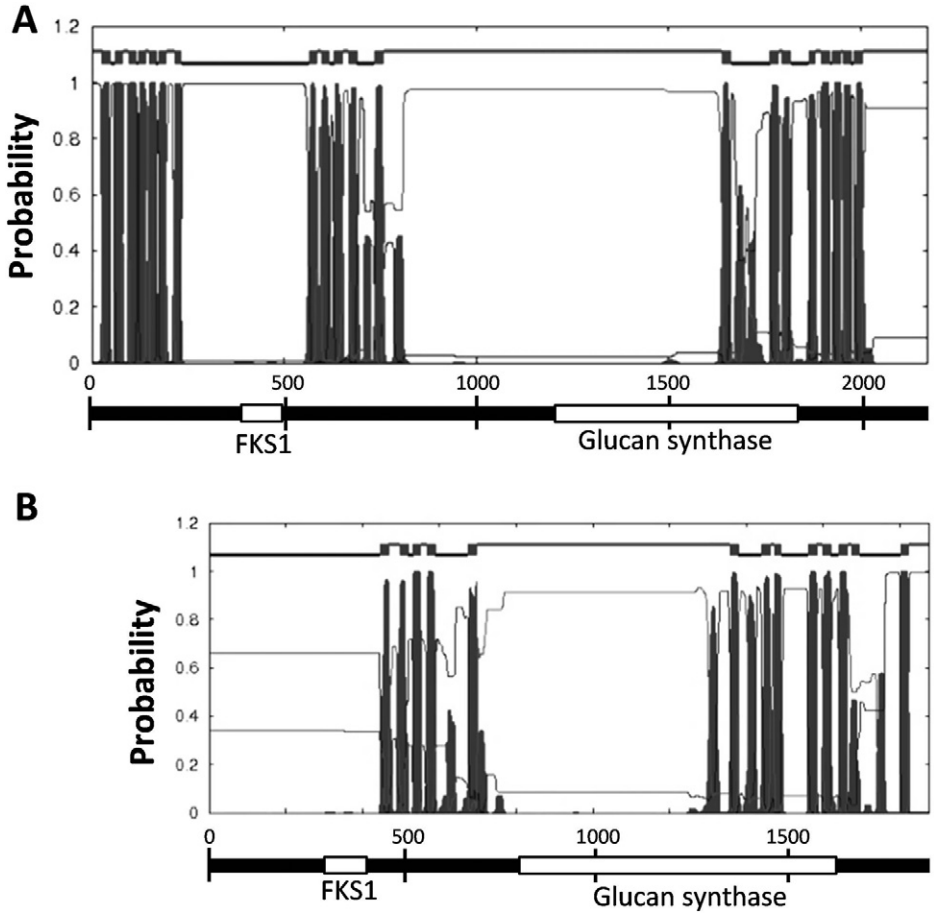

Fig. 2. Comparison of domain structure of β-1,3-glucan synthase in *T. pseudonana* and *S. cerevisiae*. Plots are TMHMM output (http://www.cbs.dtu.dk/services/TMHMM/), showing the location of predicted transmembrane segments. Below the plots are scale bar (no. of amino acids), and the location of domains in the protein.

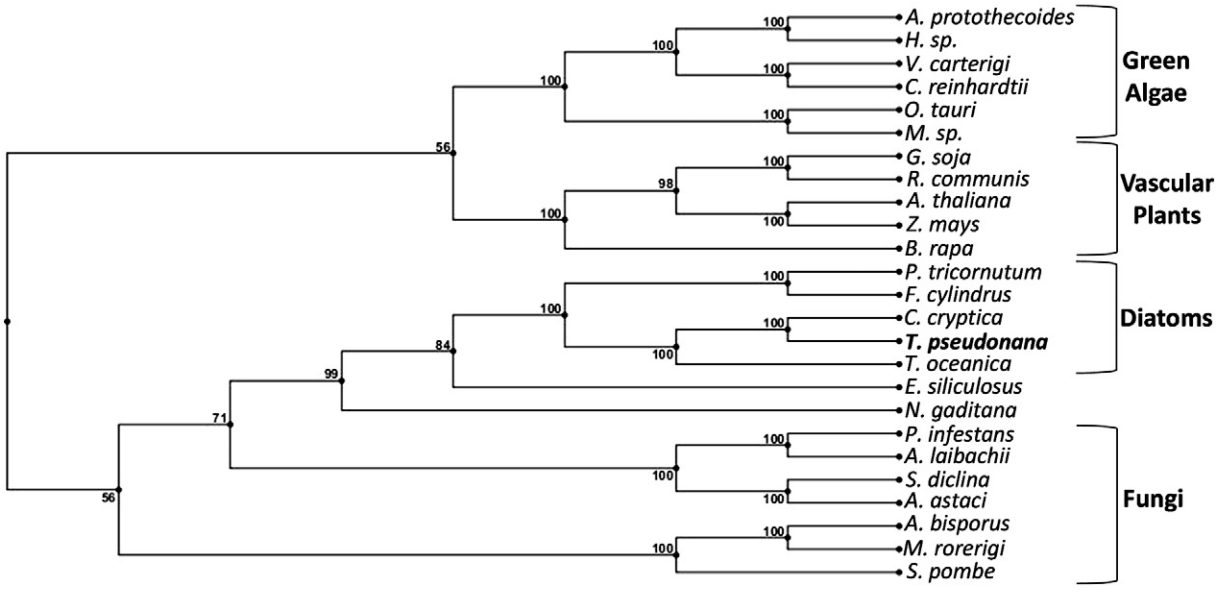

Fig. 3. Amino acid sequence comparison showing relationships among the carbohydrate synthase protein sequences from algae, plants and pathogens. The tree was generated using the CLC workbench 6 software. Bootstrap values are shown in percentages at nodes. Proteins used in the analysis were available NCBI database (*Thalassiosira pseudonana* XP_002294317.1; *Thalassiosira oceanica* EJK49176.1; *Fragilariopsis cylindrus* Fracy1_239173; *Phaeodactylum tricornutum* XP_002177442.1; *Cyclotella cryptica* g1028.t1; *Ectocarpus siliculosus*; *Galdieria sulphuraria* EME31445.1; *Cyanidioschyzon merolae* XP_005537174.1; *Micromonas* sp. XP_002500048.1; *Chlamydomonas reinhardtii* XP_001693160.1; *Helicosporidium* sp. KDD75094.1; *Auxenochlorella protothecoides* XP_011395511.1; *Volvox carteri* XP_002950451.1; *Ostreococcus tauri* CEF98660.1; *Nannochloropsis gaditana* EWM29698.1; *Ricinus communis* XP_002529727.1; *Zea mays* AFW75705.1; *Glycine soja* KHN31144.1; *Brassica rapa* XP_009118535.1; *Arabidopsis thaliana* NP_196804.6; *Albugo laibachii* CCA25481.1; *Phytophthora infestans* XP_002906408.1; *Aphanomyces astaci* XP_009835007.1; *Saprolegnia diclina* XP_008612952.1.

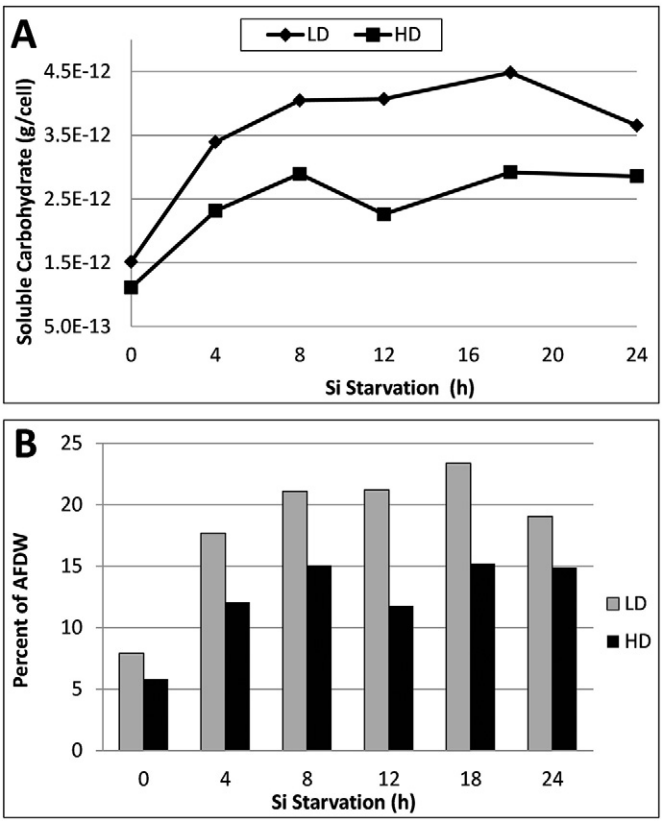

Fig. 4. Measurement of soluble carbohydrate (chrysolaminarin) levels during silicon starvation of *T. pseudonana*. A single culture was harvested and inoculated into silicon-free medium at one-half (LD) and equivalent (HD) cell density as the starter culture. A) Soluble carbohydrate per cell. B) Percent of soluble carbohydrate relative to average ash free dry weight (AFDW) of cells.

medium (Fig. 4) indicated a substantial increase within 4 h, consistent with the transcript data. To probe the response in relation to light levels, we inoculated the same starter culture into two different conditions, in one condition (LD) we inoculated silicon free medium at half the culture density as the starter, in the other (HD) we inoculated at equal density. Under both conditions, chrysolaminarin levels were induced by 4 h (Fig. 4), indicating consistency in the initial chrysolaminarin storage response. The lower density culture, which was exposed to higher light intensity per cell because of less shading, accumulated on average about 1.5 × more chrysolaminarin than the high density culture.

Transcripts for a β-1,3-exoglucanase (Thaps3_13556) and β-1,3-endoglucanase (Thaps3_1554) were upregulated maximally between 8 and 12 h silicon limitation (Fig. 1, Table S1), consistent with chrysolaminarin breakdown. Another β-1,3-endoglucanase (Thaps3_35711) was substantially downregulated (Fig. 1, Table S1). Both cytoplasmic PFKs at the unidirectional second bypass of glycolysis became upregulated at 12 h (Fig. 1, Table S1), when TAG accumulation was consistently induced [19]. Overall, the data are consistent with an initial increase in chrysolaminarin storage within 4 h of silicon limitation (Fig. 4), followed later at 12 h by breakdown of chrysolaminarin (yet maintenance of overall chrysolaminarin levels) and increased accumulation of storage lipid as TAG [19].

3.3. Knockdown of the β-1,3-glucan synthase gene, and phenotypic effects

We generated antisense-based knockdown lines of Thaps3_12695 in *T. pseudonana* in an attempt to reduce carbohydrate storage capability and evaluate the resulting effects. Since an antibody was not available to monitor protein levels for knockdown, and mRNA measurements have proven unreliable for monitoring the extent of knockdown of protein [38], we decided to screen four independent knockdown lines, with the assumption that consistent and robust phenotypic differences compared with wild-type would be indicative of reduced chrysolaminarin synthase activity.

Examination of relative chrysolaminarin content by aniline blue fluorescence microscopy [9] revealed substantially less at 24 h of silicon limitation in transgenic line CS kd-1 than wild-type (Fig. 5). The reduction in chrysolaminarin content was quantitated using imaging flow cytometry to evaluate all four knockdown lines relative to wild-type (Fig. 6). All four lines accumulated less chrysolaminarin. Averaging all together, the data indicate a 22% reduction in aniline blue fluorescence during growth (0 h) and a 54% reduction after 24 h silicon limitation (Fig. 6).

Comparison of growth rates and maximum cell density revealed possible slight, but not statistically significant, reduced growth in the knockdown lines compared with wild-type (Fig. 7). In terms of TAG accumulation, at different growth phases between wild-type and knockdown lines no differences occurred at exponential (day 1) or early stationary (day 3) phase, but a significant increase occurred (2.4-fold averaging all 4 knockdown lines, $p = 0.0006$) in stationary phase at day 5 (Fig. 8A). Comparison of TAG accumulation during silicon limitation (Fig. 8B) showed that knockdown lines accumulated 2–4.7 fold more TAG than wild-type by 24 h (mean of all four lines, 3.2 fold higher than wild-type, $p = 0.03$), but by 48 h equivalent amounts of TAG had accumulated (mean of transgenic lines, 1.01 fold higher than wild-type, $p = 0.93$). The rate of TAG accumulation varied in knockdown and wild-type lines; between 12 and 24 h, the knockdowns accumulated TAG 7.2-fold faster than wild-type, but between 24 and 48 h, wild-type accumulated 1.7-fold faster than the knockdowns.

To evaluate whether chrysolaminarin synthase knockdowns affected photosynthetic efficiency, we measured Fv/Fm values of all knockdown lines during exponential growth and after 24 h silicon limitation (Fig. 9). No significant difference was measured during exponential growth, but at 24 h silicon limitation, the knockdown lines had a slight (1.12 fold) but statistically significantly higher ($p = 0.0026$), Fv/Fm than wild-type (Fig. 9).

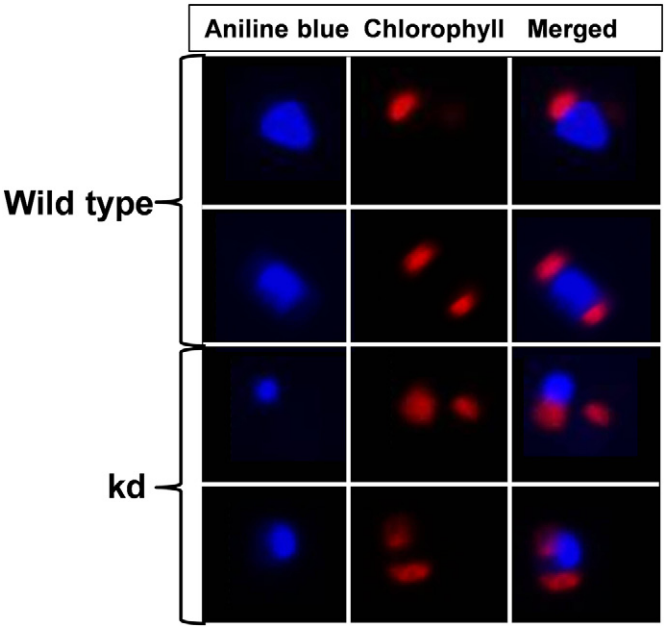

Fig. 5. Aniline blue fluorescence monitoring chrysolaminarin levels in wild type and transgenic CSkd-1 knockdown cells. Exponentially grown wild type and CS kd-1 transgenic cells were placed into silicon-free medium for 24 h. Cells were stained with aniline blue and relative fluorescence due to chrysolaminarin was visualized with a fluorescence microscope.

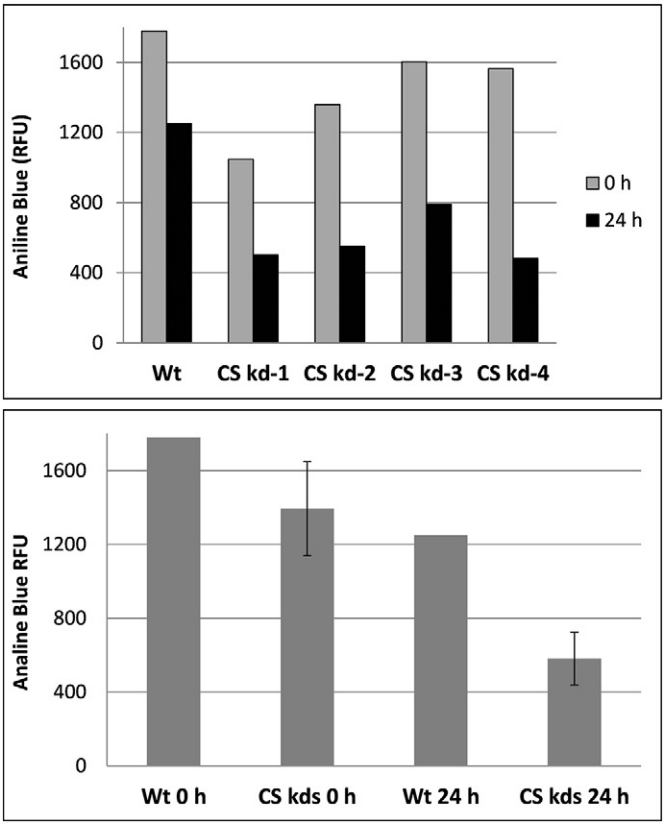

Fig. 6. Quantitation of aniline blue fluorescence in wild type and knockdown lines. Samples were analyzed by imaging flow cytometry for relative fluorescence (RFU) intensity. A) Individual lines measured at 0 and 24 h silicon limitation. B) Averages of all four transgenic knockdown (kd) lines relative to wild-type.

4. Discussion

4.1. Characteristics of the chrysolaminarin synthase

Thaps3_12695, the chrysolaminarin synthase, has conserved domains similar to fungal beta-1,3-glucan synthases (Fig. 2) and has the greatest sequence similarity with those enzymes (Fig. 3). The protein is predicted to contain an extra set of transmembrane spanning segments towards the C-terminus relative to the yeast enzyme (Fig. 2). The function of these segments is unknown, they do not match sequences other than from diatoms in BLAST searches. Given that the yeast beta-1,3-glucan synthase is localized to the plasma membrane, but the diatom enzyme is presumably localized to the vacuole, it is reasonable to assume that the extra transmembrane segments relate to either targeting or functioning of the diatom enzyme in that location. No clear targeting signal was identifiable by sequence analysis, but it is not uncommon for proteins with membrane-spanning segments near the N-terminus to mask the targeting sequence due to the hydrophobic nature of the membrane-spanning segment.

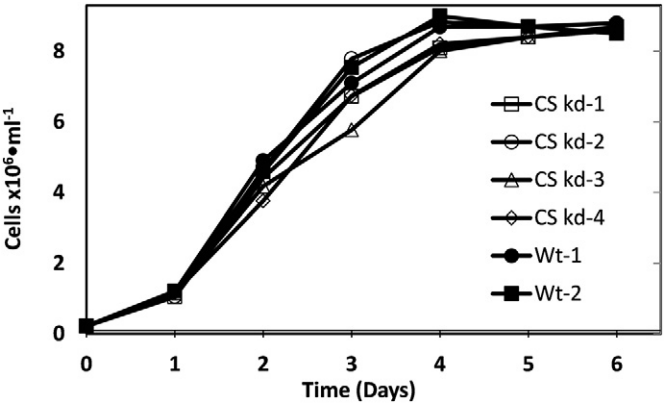

Fig. 7. Growth of wild type and transgenic cells. Wild-type and transgenic Thaps3_12695-knockdown cells were inoculated at 0.2×106 cells·ml^{-1}. Cells were grown at 18 °C under continuous light in artificial sea water (ASW). Growth was monitored by increase in number of cells. Values are means ± SE ($n = 5$).

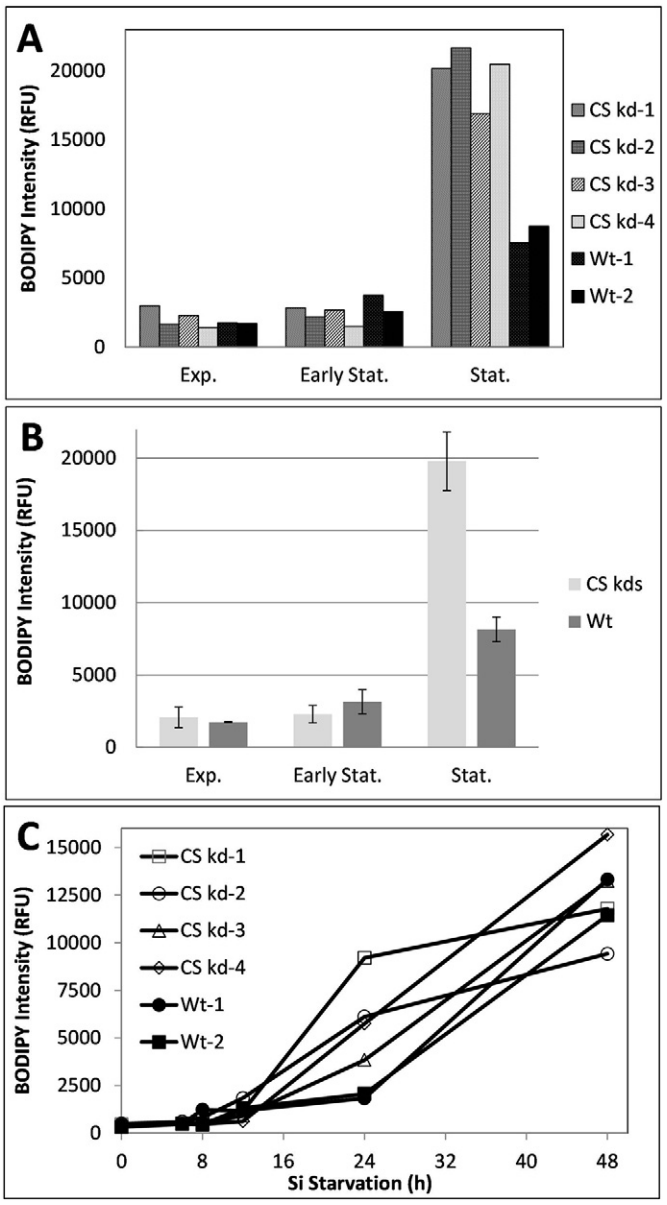

Fig. 8. Triacylglycerol (TAG) accumulation of wild type and knockdown lines. Relative fluorescence (RFU) intensity of BODIPY fluorescence was measured by imaging flow cytometry. A) TAG accumulation of individual lines at exponential (Exp.), early stationary (Early Stat.) and stationary (Stat.) phase of culturing. B) Average TAG accumulation of wild-type and transgenic lines. C) TAG accumulation of individual lines during a time course of silicon starvation.

4.2. Carbon flux processes leading to chrysolaminarin synthesis and mobilization

The overall metabolic processes in our experiments can be summarized by an initial storage of chrysolaminarin upon silicon starvation, where levels increase two-fold by 4 h (Fig. 4), followed by TAG accumulation, which reproducibly increases starting at 12 h [19]. During the

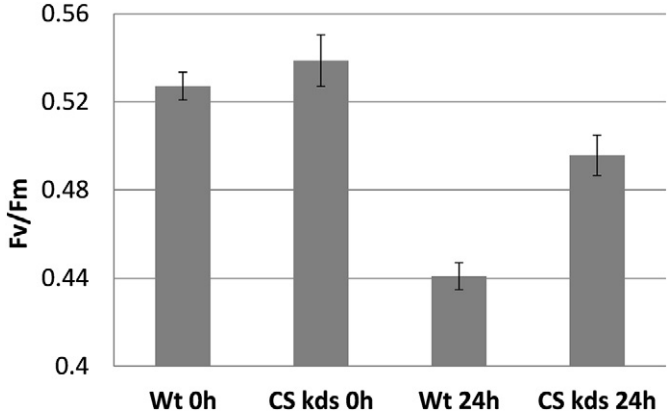

Fig. 9. Fv/Fm in wild type and transgenic Thaps3_12695 knockdown cells. Data compare exponentially growing wild type and transgenic cells with those starved for silicon for 24 h. Fv/Fm were analyzed in dark adapted cells.

TAG accumulation process, transcript data suggest that chrysolaminarin is broken down and processed through cytoplasmic glycolysis (Fig. 1). During this time, chrysolaminarin stores remain high, and are not depleted throughout the time course (Fig. 4).

The initial increase in chrysolaminarin followed by subsequent mobilization is similar to what was determined in pulse chase radiolabeling experiments done during nitrogen limitation in the diatom *Skeletonema costatum*. Label was incorporated to the extent of 85% into β-1,3-glucan within 4 h of nitrogen limitation, and amino acids became labeled later during the chase period [17], suggesting initial rapid storage of fixed carbon into carbohydrate followed by mobilization of carbohydrate into biochemical intermediates. Work by Roessler [16] examined labeling of chrysolaminarin and lipid during silicon starvation in *Cyclotella cryptica*, with apparently conflicting results. Initial pulse labeling indicated a preferential partitioning of label into lipid and a decrease of label into chrysolaminarin over time. However, a chase experiment indicated a reduction of label in chrysolaminarin and an increase into lipid, consistent with mobilization of the carbohydrate store into lipid. This might be interpreted as an initial direct labeling of lipid, bypassing the chrysolaminarin storage step, however, another possibility is that chrysolaminarin levels were high to begin with, in which case the ability to increase labeling of the chrysolaminarin pool could have been minimal, and most label would appear in the lipid fraction. In the Roessler study, in contrast to Granum and Myklestad [17] and our work, cultures were bubbled with 1% CO_2. We can speculate that increased carbon input under these conditions could lead to an increased chrysolaminarin level at the outset, however, since absolute chrysolaminarin levels were not measured in the Roessler study, an unambiguous resolution is not possible.

The transcriptomic data indicates that both chloroplast and cytoplasmic gluconeogenesis are induced by 4 h after silicon starvation (Fig. 1). In the chloroplast, gluconeogenesis is likely the only direction of carbon flux because a chloroplast-targeted PFK at the second bypass step is missing [39], preventing flux in the glycolytic direction. Many gluconeogenic steps in the chloroplast are also involved in the Calvin-Benson cycle. We documented that RubisCO small and large subunit transcripts are upregulated maximally at a later time point and with a different pattern [19] than the induction of transcripts for the gluconeogenic steps at 4 h (Fig. 1), thus the gluconeogenic upregulation appears to be related to carbon flux towards glucose-1-phosphate (G-1-P) in the chloroplast. The data suggest that two different carbon compounds may be exported from the chloroplast and eventually used for chrysolaminarin synthesis, G-1-P generated by the chloroplast PGMase (Thaps3_35878), and 3-phosphoglycerate (3PG), a direct product of carbon fixation by RubisCO (Fig. 1). The latter is supported by a recent flux analysis in *P. tricornutum* [40].

Questions to consider are: what are the relative fluxes of carbon through chloroplast and cytoplasmic gluconeogenesis and do they vary during the time course? Labeled flux analysis is required to directly answer that question, which was beyond the scope of this study, but there are relevant observations from the data on hand. We observed that by averaging the responses of all upregulated transcripts, the relative expression pattern of the upregulated genes in the chloroplast and cytoplasm were identical, with a precise ratio of 2:1, with the exception of the 12 h time point, where the ratio was precisely 1:1 (Fig. 10). This should not be interpreted as being indicative of the relative flux in each compartment, however the exactness of the ratios indicates coordinate control between compartments. Chrysolaminarin pools are essentially filled by 8 h during Si starvation, and remain high for the duration of the experiment (Fig. 4). Eight hours is when gluconeogenic transcript levels decrease after the 4 h maximum (Fig. 10). Even though transcript levels are reduced, they do not return to pre-starvation levels (Fig. 10). We interpret this to suggest that after an initial filling of chrysolaminarin pools to high levels, continued synthesis of chrysolaminarin occurs as the pools are simultaneously depleted for other processes. In our experiments, this specifically means fatty acid synthesis, which particularly increases as TAG begins to accumulate at 12 h [19]. Because transcripts for both chloroplast and cytoplasmic glycolysis/gluconeogenesis remain upregulated after 12 h, with the same ratio between them, this suggests that both pathways are still operating after chrysolaminarin pools are filled, and that fatty acid synthesis in the chloroplast does not affect gluconeogenic carbon flux in that organelle. The reason for the relative downregulation of chloroplast transcripts at 12 h is unclear, but it obviously correlates with the beginning of the period of TAG accumulation.

Chrysolaminarin stores constitute a considerable portion of cell mass, in our experiments between 5.8 and 23.4% of ash free dry weight (AFDW - Fig. 4). By comparison, in a previous study fatty acids (measured as FAME) increased from 3.6–10.4% of AFDW during 24 h silicon starvation [19]. In a different study using a gradual silicon starvation regime [18], fatty acids accumulated up to 18%.

4.3. Effect of knockdowns

We used an antisense approach to knock down Thaps3_12695 expression. We previously documented no correlation between transcript level changes generated by either antisense or RNAi knockdowns and resulting protein levels – in some cases, increased transcript was present in knockdown lines relative to wild-type, but substantial reduction in protein levels occurred [38]. This could be due to translation-inhibition effects of knockdown combined with an attempt by the cell to compensate by increasing mRNA levels. Thus, monitoring transcript levels in knockdown lines is not necessarily indicative of the extent of protein knockdown. We lacked an antibody against the chrysolaminarin synthase, which necessitated a phenotypic screen for reduced

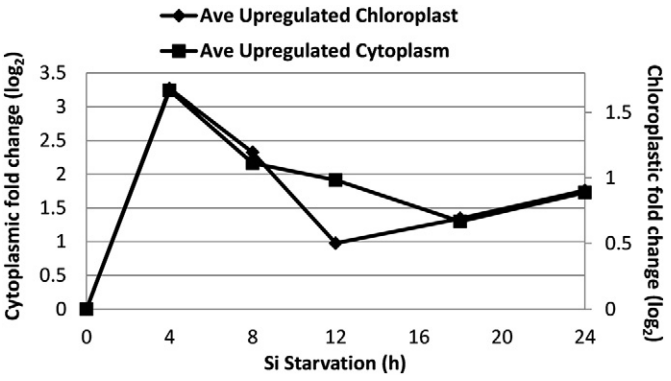

Fig. 10. Relative change in transcript levels averages over all upregulated chloroplast and cytoplasmic genes during the time course of silicon starvation.

chrysolaminarin in knockdown lines. The rationale behind this was that if a consistent phenotype was observed in all knockdown lines, the phenotype would correlate with the genotype, which is conceptually similar to a classical genetic screen. Some variability, which we do observe, should be expected based on insertion effects of the knockdown construct into different genomic locations.

All four knockdown lines had reduced chrysolaminarin content (by 22% on average) relative to wild-type during growth, which was accentuated to 54% after 24 h silicon starvation (Fig. 6). In terms of growth rate (Fig. 7), three of the four lines appeared to have slightly less growth during late exponential/early stationary phase, but these differences were not statistically significant, therefore any effect was slight.

4.4. Relationship between growth and carbon storage

The data in Figs. 4, 7, and 8 indicate a relationship between growth rate, chrysolaminarin and TAG levels, as well as the timing of growth cessation under silicon starvation. The knockdowns had no effect on TAG levels during exponential or early stationary phase growth, but TAG was increased by 2.4-fold in stationary phase (Fig. 8). During silicon starvation, there was no significant difference in TAG between the knockdowns and wild-type except at 24 h, where 3.2-fold higher TAG was present on average in the knockdown lines (Fig. 8). These data suggest that the effect of chrysolaminarin levels on TAG accumulation is triggered by growth cessation and is transient. The data suggest that a tradeoff occurs comparing the knockdown lines with wild-type between the rate of generation of photosynthate relative to the ability to store it in different forms. Even though chrysolaminarin storage could occur over a longer period of time in the knockdown lines (which presumably have less chrysolaminarin synthesis activity), eventually catching up with wild-type, the rate of production of photosynthate outstrips the ability to store that carbon as chrysolaminarin, and it is shuttled into the alternative carbon storage form, TAG, more rapidly on the short term. This is consistent with TAG accumulation being considered an "overflow" mechanism that is dependent on chrysolaminarin levels, and not the ability to store chrysolaminarin at a particular rate.

One question to address is whether the increased chrysolaminarin content during growth cessation is due to less utilization of chrysolaminarin, or increased flux of carbon into chrysolaminarin stores. The induction of transcripts for chrysolaminarin synthesis in wild-type during silicon starvation suggests an increased flux into storage, suggesting that the cell is not maximizing storage carbohydrate levels during growth. The effect of knockdown on chrysolaminarin levels is greater under growth cessation relative to growth (Fig. 6), which is also consistent with cells not maximizing chrysolaminarin pools during growth. This may seem surprising, because energy and carbon demands for cell division might be expected to be high, and more chrysolaminarin would need to be available during that time. An alternative explanation is that diatoms may not solely rely on storage carbohydrate for growth processes (see below) and because energy and carbon outlets are restricted during growth cessation, storing additional carbon as chrysolaminarin (and eventually lipid) provides an energy, reducing equivalent, and biochemical sink for photosynthesis, as has been proposed in general for microalgae [41].

The Fv/Fm data (Fig. 9) suggest that accumulation of chrysolaminarin has a slight negative effect on photosynthetic efficiency. If we consider the hypothesis that chrysolaminarin stores serve as a sink for photosynthesis, then increased stores should have a negative effect. This is based on the generally observed correlation between chlorophyll fluorescence parameters and CO_2 assimilation due to the direct use in known ratios of products of linear electron transport, ATP and NADPH, in photosynthetic carbon assimilation [42].

The transient increase in TAG at 24 h in knockdown lines under silicon starvation relative to wild-type can be explained as follows. TAG accumulation does not occur until 12 h [19], therefore carbon flux into TAG will be limited for both wild-type and knockdowns up until that time. By 24 h, the reduced ability to store chrysolaminarin could enhance the rate of TAG accumulation in knockdown lines – less carbon can be accommodated by the chrysolaminarin pools, which gets shuttled into TAG. During the subsequent 24 h, in wild-type and the knockdowns equilibrium could be reached between carbon flux into and out of chrysolaminarin pools. If we assume roughly similar amounts of photosynthate being produced over the entire 48 h period for both wild-type and knockdowns, then the overall amount of TAG should become similar once chrysolaminarin pools become equilibrated. Basically, chrysolaminarin pools become saturated faster in the knockdowns compared with wild-type and the excess available carbon is shuttled into TAG earlier, but if over time, carbon fixation is similar between the two, eventually TAG accumulation will be equivalent.

Similarities are found by comparing our data with knockdowns or knockouts of the cytoplasmic UGPase/PGMase genes in *P. tricornutum*. Zhu et al. [26] grew both antisense and RNAi knockdown lines under 12:12 L:D conditions. Unfortunately, the authors did not report at what time of day measurements were made, but on average the knockdown lines exhibited about a 3% reduction in growth rate, a 48% reduction in chrysolaminarin, and a 10% increase in total cellular lipids [26]. Experiments on a TALEN-based knockout line for the UGPase/PGMase gene in *P. tricornutum* did not report on changes in chrysolaminarin nor growth rate, but showed about a 3-fold increase in TAG under nitrogen starvation [27]. We see a similar slight reduction in growth rate and generally similar reduction in chrysolaminarin content in the chrysolaminarin synthase knockdown lines, with a transient 3-fold increase in TAG at 24 h silicon starvation (Figs. 6-8). Thus, knockdown of the two genes sequentially involved in chrysolaminarin synthesis result in consistent phenotypic effects.

4.5. Comparison with green algae

There is a general observation in diverse green algal species and also diatoms that fixed carbon is processed through storage carbohydrate first, followed by utilization of carbohydrate for TAG [16,43–45], but the consequences of reducing carbohydrate storage in different algal classes are quite different.

Starchless mutants of green algae have been observed to accumulate higher levels of TAG under particular, but not all, nutrient limited conditions [43,46–49]. In *Chlamydomonas reinhardtii* the *sta6* mutant has a defective ADP-glucose pyrophosphorylase (AGPase) which catalyzes a similar step as UGPase in diatoms, generating the immediate precursor for storage carbohydrate synthesis. The *sta6* mutant grown under autotrophic conditions in continuous light with ambient levels of CO_2 had a 30% longer doubling time, about one-third less maximum culture density, and dry cell weights 20–35% less than wild-type [48]. At stationary phase, total reducing carbohydrate was 2–5 times lower than in wild-type, but there were not significant increases in protein or lipid, indicating that repartitioning of carbon was not occurring. Thus, the *sta6* mutation impedes carbon assimilation into all biopolymers. In that study, TAG accumulation only occurred in the presence of acetate. Photosynthetic parameters (O_2 evolution, electron transport rate) were negatively affected at higher light intensities in the mutant, non-photochemical quenching was not. *Sta6* had a slightly lower Fv/Fm, and exhibited attenuated rates of NADPH re-oxidation because gluconeogenic carbon flux towards starch synthesis was inhibited, with a corresponding accumulation of metabolic intermediates [48].

The data on *sta6* described in the previous paragraph was obtained on cultures grown under ambient CO_2, which resulted in no TAG accumulation, however in another study when cultures were incubated with 5% CO_2, TAG accumulation occurred under nitrogen starvation [49]. TAG accumulation initially occurred at a much faster rate in the mutant, but towards the end of the experiment the rate in wild-type was faster [49]. This is similar to our observation that TAG accumulation in wild-type eventually caught up with the knockdowns (Fig. 8). The growth rate of *sta6* in acetate containing medium has been reported

as equivalent to wild-type, and TAG accumulation also occurs with acetate under nitrogen starvation [47–49].

A starchless mutant with an unknown genotype has been characterized in *Scenedesmus obliquus* [50]. Under autotrophic conditions, the slm1 mutant grew less rapidly and to lower culture density and total biomass than wild-type, and under nitrogen starvation, accumulated TAG more rapidly but to similar maximum levels as wild-type, without the need for acetate or CO_2 supplementation. In wild-type, TAG began accumulating after starch began to be consumed. Fv/Fm in the mutant was similar to or slightly higher than in wild-type. Thus, overall photosynthetic performance was not seriously altered, but there was an improved partitioning of carbon towards TAG in the mutant. Comparison with the sta6 mutant in *C. reinhardtii* suggests that the ability to partition carbon differs between the two species under autotrophic conditions. The carbon partitioning differences, which are likely related to the complement and intracellular location of carbon flux enzymes and/or intercompartmental transport processes [3,39], may help define what makes an oleaginous and non-oleaginous strain.

Comparison of the responses of chrysolaminarin knockdowns in *T. pseudonana* with starchless mutants in *C. reinhardtii* and *S. obliquus* raise questions about how carbohydrate storage in different cellular locations relates to photosynthesis, growth, and TAG accumulation. In green algae, it has been proposed that the evolution of light harvesting complexes (LHCs) which substituted for phycobilisomes from the original cyanobacterial endosymbiont might have facilitated the return of storage carbohydrate into the plastid due to the need for a plastidial source of ATP at night for chlorophyll synthesis [51]. The downside of this arrangement is that both gluconeogenic and glycolytic fluxes would occur in the chloroplast, which could be considered inefficient or require a higher degree of regulatory control if both processes occur simultaneously. Green algae have addressed this issue by synthesizing starch in the light, which consumes ATP and NADPH available from photosynthesis processes, and then generally (but not exclusively) breaking down starch in the dark to generate energy and reducing equivalents. Consistent with this is the observation that transcript levels and enzymatic activity for ADP-glucose pyrophosphorylase increase during the daytime and decrease at night [52]. Thus, the gluconeogenic and glycolytic processes are separated temporally. Green algae cultured under light:dark conditions tend to not to divide in the light, but commonly divide shortly after the dark period begins [53–57]. Dark conditions, or the application of the photosynthesis inhibitor DCMU, increase starch degradation [55,58], indicating that the status of photosynthesis influences the net direction of carbon flux. Even when division occurs in the light, energy required for mitosis results from starch breakdown [53,59]. The starchless mutants for both *C. reinhardtii* and *S. obliquus* exhibited poorer growth than wild-type, consistent with the involvement of starch for generation of growth energy [48,50].

Because diatoms lack chloroplast targeted PFKs, net carbon flux in that organelle must occur in the gluconeogenic direction. The unidirectionality, as well as the location of carbohydrate storage outside of the chloroplast, is likely to simplify the regulation of chloroplast carbon flux relative to green algae. One concept to consider relates to the involvement of several gluconeogenic intermediates also participating in the Calvin Benson cycle. In *C. reinhardtii*, blockage of starch storage results in a buildup of these intermediates, which could negatively affect carbon fixation [48]. A diatom would have the option of exporting G-1-P from the chloroplast regardless of whether chrysolaminarin storage was inhibited, and this export could act as an overflow valve if excess carbon relative to Calvin Benson cycle needs was generated. It is therefore possible that negative feedback into the Calvin Benson cycle could be minimized or avoided.

In contrast to the green algae, diatoms tend to divide during the light period [60–65]. Under daylight conditions, it seems likely that energy and carbon required for division can be met to a greater extent from photosynthetic processes than to storage carbohydrate in a diatom. Consistent with this, recent flux analysis suggests that 3PG is preferentially exported over glucose-1-phosphate from the chloroplast under autotrophic conditions in *P. tricornutum* [43]. Because ATP and NAD(P)H is required for carbohydrate storage, daytime mitosis that relies more directly on photosynthesis should reduce overall energy drains on the cell related to the synthesis and breakdown of carbohydrate. The observation that chrysolaminarin pools are not maximized during growth (Fig. 4) suggests that chrysolaminarin is not an exclusive source for energy generation for cell division. Also consistent with these concepts is an observation that cellular carbohydrate levels fluctuate relatively little during diurnal cycles [66]. In contrast, in *C. reinhardtii* starch levels have been documented to increase to a maximum until the end of the light period [55,59]. Growth was not substantially inhibited in our knockdown lines (Fig. 7), which could either suggest a lesser reliance on carbohydrate stores for growth in diatoms, or a lesser reduction of chrysolaminarin comparing our knockdown approach with the knockout approaches used to generate starchless mutants [48,50]. Indeed, *sta6* starch levels were below detectable limits, on the order of 0.1% of the wild-type starch content [52].

Considering the above discussion, the ease with which fatty acids and TAG can accumulate should differ in relation to light and dark periods in the different classes of microalgae. In *C. reinhardtii*, net breakdown of starch occurs at night, suggesting that fatty acid synthesis and TAG accumulation could preferentially occur then. That is consistent with nighttime division, fatty acids for membrane lipids for daughter cells would have to be synthesized for mitosis. The drawback of performing FA and TAG synthesis at night is the lack of incoming energy from photosynthesis, which may suggest a greater reliance on carbohydrate, which would translate into a need for higher carbohydrate levels as starch being stored in green algae. Comparing cellular starch levels under nitrogen limitation in *C. reinhardtii* [58] with chrysolaminarin levels under silicon starvation in *T. pseudonana* (Fig. 4), indicates on the order of 17.7 fold higher carbohydrate per cell by weight in *C. reinhardtii*, or in terms of percent of cell weight, storage carbohydrate constitutes 23.4% in the diatom (Fig. 4) and 49% in *C. reinhardtii* [58,67].

Our data suggest that reduction of chrysolaminarin storage in *T. pseudonana* can result in increases in TAG accumulation, but these may be transient (Fig. 8). If similar results hold for strains of diatoms being considered for lipid-based biofuel production, then choosing an appropriate time to harvest will be essential to maximize yields.

The presented data examine the processes of carbon flux relative to chrysolaminarin storage in a diatom, and the effects of reducing chrysolaminarin storage on growth and TAG accumulation. The apparent lesser reliance on storage carbohydrate for energy generation during cell division, as suggested in this and other studies [40], may provide clues for the generally high productivity of diatoms.

Supplementary data to this article can be found online at http://dx.doi.org/10.1016/j.algal.2017.01.010.

Acknowledgements

The research was supported by Air Force Office of Scientific Research (AFOSR) grants FA9550-08-1-0178 and FA9550-08-1- 0178, US Department of Energy grants DE-EE0001222, DEEE0003373 and DE-SC0012556, National Science Foundation grant CBET-0903712, California Energy Commission's 'California Initiative for Large Molecule Sustainable Fuels', agreement number: 500-10-039.

References

[1] J.A. Raven, Cellular location of starch synthesis and evolutionary origin of starch genes, J. Phycol. 41 (2005) 1070–1072.
[2] S. Ball, C. Colleoni, U. Cenci, J.N. Raj, C. Tirtiaux, The evolution of glycogen and starch metabolism in eukaryotes gives molecular clues to understand the establishment of plastid endosymbiosis, J. Exp. Bot. 62 (2011) 1775–1801.
[3] M. Hildebrand, R.M. Abbriano, J.E.W. Polle, J.C. Traller, E.M. Trentacoste, S.R. Smith, A.K. Davis, Metabolic and cellular organization in evolutionarily diverse microalgae as related to biofuels production, Curr. Opin. Chem. Biol. 17 (2013) 506–514.

[4] R.G. Dorrell, A.G. Smith, Do red and green make brown? Perspectives on plastid acquisitions within chromalveolates, Eukaryot. Cell 10 (2011) 856–868.
[5] P.G. Falkowski, M.E. Katz, A.H. Knoll, A. Quigg, J.A. Raven, O. Schofield, F.J.R. Taylor, The evolution of modern eukaryotic phytoplankton, Science 305 (2004) 354–360.
[6] L.R. Kump, The rise of atmospheric oxygen, Nature 451 (2008) 277–278.
[7] J.A. Raven, M. Giordano, J. Beardall, S.C. Maberly, Algal evolution in relation to atmospheric CO_2: carboxylases, carbon concentrating mechanisms and carbon oxidation cycles, Philos. Trans. R. Soc. B 367 (2012) 493–507.
[8] A. Chiovitti, P. Molino, S.A. Crawford, R.W. Teng, T. Spurck, R. Wetherbee, The glucans extracted with warm water from diatoms are mainly derived from intracellular chrysolaminarin and not extracellular polysaccharides, Eur. J. Phycol. 39 (2004) 117–128.
[9] L. Waterkeyn, A. Bienfait, Localisation et role des b-1,3-glucanes (callose et chrysolaminarine) dans le genre Pinnularia (Diatome'es), Cellule 74 (1987) (1987) 198–226.
[10] R.A. Andersen, *Ochromonas moestrupii* sp. nov. (Chrysophyceae), a new golden flagellate from Australia, Phycologia 50 (2011) 600–607.
[11] S.M. Myklestad, Production, chemical structure, metabolism, and biological function of the (1 → 3)-linked, β3-D-glucans in diatoms, Biol. Oceanogr. 6 (1989) 313–326.
[12] Z. Ju, L. Ding, Q. Zheng, Z. Wu, F. Zheng, Diatoms as a model system in studying lipid biosynthesis regulation, Int. J. Environ. Sci. Devel. 2 (2011) 493–495.
[13] S. Xia, G. Song, L. Baoyan, A.F. Li, J.H. Xiong, Z.Q. Ao, C.W. Zhang, Preliminary characterization, antioxidant properties and production of chrysolaminarin from marine diatom *Odontella aurita*, Mar. Drugs 12 (2014) 4883–4897.
[14] K.M. Varum, S. Myklestad, Effects of light, salinity and nutrient limitation on the production of b-1,3-D-Glucan and Exo-D-Glunanase activity in *Skeletonema costatum* (Grev.) Cleve, J. Exp. Mar. Biol. Ecol. 83 (1984) 13–25.
[15] J. Fettke, M. Hejazi, J. Smirnova, E. Hochel, M. Stage, M. Steup, Eukaryotic starch degradation: integration of plastidial and cytosolic pathways, J. Exp. Bot. 60 (2009) 2907–2922.
[16] P.G. Roessler, Effects of silicon deficiency on lipid composition and metabolism in the diatom *Cyclotella cryptica*, J. Phycol. 24 (1988) 394–400.
[17] E. Granum, S.M. Myklestad, Mobilization of beta-1,3-glucan and biosynthesis of amino acids induced by NH4+ addition to N-limited cells of the marine diatom *Skeletonema costatum* (Bacillariophyceae), J. Phycol. 37 (2001) 772–782.
[18] E.T. Yu, F.J. Zendejas, P.D. Lane, S. Gaucher, B.A. Simmons, T.W. Lane, Triacylglycerol accumulation and profiling in the model diatoms *Thalassiosira pseudonana* and *Phaeodactylum tricornutum* (Baccilariophyceae) during starvation, J. Appl. Phycol. 21 (2009) 669–681.
[19] S.R. Smith, C. Glé, R.M. Abbriano, J.C. Traller, A. Davis, E. Trentacoste, M. Vernet, A.E. Allen, M. Hildebrand, Transcript level coordination of carbon pathways during silicon starvation-induced lipid accumulation in the diatom *Thalassiosira pseudonana*, New Phytol. 2016 (2016)http://dx.doi.org/10.1111/nph.13843.
[20] P.G. Roessler, Changes in the activities of various lipid and carbohydrate biosynthetic enzymes in the diatom *Cyclotella cryptica* in response to silicon deficiency, Arch. Biochem. Biophys. 267 (1998) 521–528.
[21] P.G. Roessler, UDPglucose pyrophosphorylase activity in the diatom *Cyclotella cryptica* – pathway of chrysolaminarin biosynthesis, J. Phycol. 23 (1987) 494–498.
[22] E. Granum, S. Kirkvold, S.M. Myklestad, Cellular and extracellular production of carbohydrates and amino acids by the marine diatom *Skeletonema costatum*: diel variations and effects of N depletion, Mar. Ecol. Prog. Ser. 242 (2002) 83–94.
[23] J. Sheehan, T. Dunahay, J. Benemann, P. Roessler, A Look Back at the U.S. Department of Energy's Aquatic Species Program: Biodiesel from Algae, http://www.nrel.gov/biomass/pdfs/24190.pdf 1998.
[24] P.G. Kroth, A. Chiovitti, A. Gruber, V. Martin-Jezequel, T. Mock, M.S. Parker, M.S. Stanley, A. Kaplan, L. Caron, T. Weber, et al., A model for carbohydrate metabolism in the diatom *Phaeodactylum tricornutum* deduced from comparative whole genome analysis, PLoS One 3 (2008), e1426.
[25] W. Huang, C.R. Bartulos, P.G. Kroth, Diatom vacuolar 1,6-beta-transglycosylases can functionally complement the respective yeast mutants, J. Eukaryot. Microbiol. 63 (2016) 536–546.
[26] B.H. Zhu, H.P. Shi, G.P. Yang, N.N. Lv, M. Yang, K.H. Pan, Silencing UDP-glucose pyrophosphorylase gene in *Phaeodactylum tricornutum* affects carbon allocation, New Biotechnol. 33 (2016) 237–244.
[27] F. Daboussi, S. Leduc, A. Marechal, et al., Genome engineering empowers the diatom *Phaeodactylum tricornutum* for biotechnology, Nat. Commun. 5 (2014) Article Number: 3831.
[28] W.M. Darley, B.E. Volcani, Role of silicon in diatom metabolism. A silicon requirement for deoxyribonucleotide synthesis in the diatom *Cylindrotheca fusiformis*, Exp. Cell Res. 58 (1969) 334–342.
[29] N. Poulsen, P.M. Chesley, N. Kroger, Molecular genetic manipulation of the diatom *Thalassiosira pseudonana* (Bacillariophyceae), J. Phycol. 42 (2006) 1059–1065.
[30] T. Govender, L. Ramanna, I. Rawat, F. Bux, BODIPY staining, an alternative to the Nile Red fluorescence method for the evaluation of intracellular lipids in microalgae, Bioresour. Technol. 114 (2012) 507–511.
[31] M.S. Cooper, W.R. Hardin, T.W. Petersen, R.A. Cattolico, Visualizing "green oil" in live algal cells, J. Biosci. Bioeng. 109 (2010) 198–201.
[32] J.C. Traller, M. Hildebrand, High throughput imaging to the diatom *Cyclotella cryptica* demonstrates substantial cell-to-cell variability in the rate and extent of triacylglycerol accumulation, Algal Res. 2 (2013) 244–252.
[33] O. Emanuelsson, H. Nielsen, G. von Heijne, ChloroP, a neural network-based method for predicting chloroplast transit peptides and their cleavage sites, Protein Sci. 8 (1999) 978–984.
[34] D. Moog, S. Stork, S. Zauner, U.G. Maier, In silico and in vivo investigations of proteins of a minimized eukaryotic cytoplasm, Genome Biol. Evol. 3 (2011) 375–382.
[35] H. Okada, M. Abe, M. Asakawa-Minemura, et al., Multiple functional domains of the yeast l,3-beta-glucan synthase subunit Fks1p revealed by quantitative phenotypic analysis of temperature-sensitive mutants, Genetics 184 (2010) 1013–1024.
[36] T. Roemer, S. Delaney, H. Bussey, SKN1 and KRE6 define a pair of functional homologs encoding putative membrane proteins involved in beta-glucan synthesis, Mol. Cell. Biol. 13 (1993) 4039–4048.
[37] R. Timpl, D. Tisi, J.F. Talts, Z. Andac, T. Sasaki, E. Hohenester, Structure and function of laminin LG modules, Matrix Biol. 19 (2000) 309–317.
[38] R.P. Shrestha, M. Hildebrand, Evidence for a regulatory role of diatom silicon transporters in cellular silicon responses, Eukaryot. Cell 14 (2015) 29–40.
[39] S.R. Smith, R.M. Abbriano, M. Hildebrand, Comparative analysis of diatom genomes reveals substantial differences in the organization of carbon partitioning pathways, Algal Res. 1 (2012) 2–16.
[40] J. Kim, M. Fabris, G. Baart, M.K. Kim, A. Goossens, W. Vyverman, P.G. Falkowski, D.S. Lun, Flux balance analysis of primary metabolism in the diatom *Phaeodactylum tricornutum*, Plant J. 85 (2016) 161–176.
[41] Q. Hu, M. Sommerfeld, E. Jarvis, M. Ghirardi, M. Posewitz, M. Seibert, A. Darzins, Microalgal triacylglycerols as feedstocks for biofuel production: perspectives and advances, Plant J. 54 (2008) 621–639.
[42] E.H. Murchie, T. Lawson, Chlorophyll fluorescence analysis: a guide to good practice and understanding some new applications, J. Exp. Bot. 64 (2013) 3983–3998.
[43] Y. Li, D. Han, G. Hu, D. Dauvillee, M. Sommerfeld, S. Ball, Q. Hua, *Chlamydomonas* starchless mutant defective in ADP-glucose pyrophosphorylase hyper-accumulates triacylglycerol, Metab. Eng. 12 (2010) 387–391.
[44] J. Msanne, D. Xu, A.R. Konda, J.A. Casas-Mollano, T. Awada, E.B. Cahoon, H. Cerutti, Metabolic and gene expression changes triggered by nitrogen deprivation in the photoautotrophically grown microalgae *Chlamydomonas reinhardtii* and Coccomyxa sp. C-169, Phytochemistry 75 (2012) 50–59.
[45] S. Zhu, W. Huang, J. Xu, Z. Wang, J. Xu, Z. Yuan, Metabolic changes of starch and lipid triggered by nitrogen starvation in the microalga Chlorella zofingiensis, Bioresour. Technol. 152 (2013) 292–298.
[46] V.H. Work, R. Radakovits, R.E. Jinkerson, et al., Increased lipid accumulation in the *Chlamydomonas reinhardtii* sta7-10 starchless isoamylase mutant and increased carbohydrate synthesis in complemented strains, Eukaryot. Cell 9 (2010) 1251–1261.
[47] Z.T. Wang, N. Ullrich, S. Joo, S. Waffenschmidt, U. Goodenough, Algal lipid bodies: stress induction, purification, and biochemical characterization in wild-type and starchless *Chlamydomonas reinhardtii*, Eukaryot. Cell 8 (2009) 1856–1868.
[48] A. Krishnan, G.K. Kumaraswamy, D.J. Vinyard, H.Y. Gu, G. Ananyev, M.C. Posewitz, G.C. Dismukes, Metabolic and photosynthetic consequences of blocking starch biosynthesis in the green alga *Chlamydomonas reinhardtii* sta6 mutant, Plant J. 81 (2015) 947–960.
[49] M.P. Davey, I. Horst, G.H. Duong, E.V. Tomsett, A.C.P. Litvinenko, C.J. Howe, A.G. Smith, Triacylglyceride production and autophagous tesponses in *Chlamydomonas reinhardtii* depend on resource allocation and carbon source, Eukaryot. Cell 13 (2014) 392–400.
[50] G. Breuer, L. de Jaeger, V.P.G. Artus, D.E. Martens, J. Springer, R.B. Draaisma, G. Eggink, R.H. Wijffels, P.P. Lamers, Superior triacylglycerol (TAG) accumulation in starchless mutants of *Scenedesmus obliquus*: (II) evaluation of TAG yield and productivity in controlled photobioreactors, Biotech. Biofuels 7 (2014) http://dx.doi.org/10.1186/1754-6834-7-70 Article Number: 70.
[51] P. Deschamps, I. Haferkamp, C. d'Hulst, H.E. Neuhaus, S.G. Ball, The relocation of starch metabolism to chloroplasts: when, why and how, Trends Plant Sci. 13 (2008) 574–582.
[52] C. Zabawinski, N. Van den Koornhuyse, C. D'Hulst, R. Schlichting, C. Giersch, B. Delrue, J.M. Lacroix, J. Preiss, S. Ball, Starchless mutants of *Chlamydomonas reinhardtii* lack the small subunit of a heterotetrameric ADP-glucose pyrophosphorylase, J. Bacteriol. 183 (2001) 1069–1077.
[53] F. Wanka, M.M.J. Joppen, Ch.M.A. Kuyper, Starch degrading enzymes in synchronous cultures of *Chlorella*, Z. Pflanzenphysiol. 62 (1970) 146–157.
[54] S. Lemaire, M. Hours, C. Gerard-Hirne, A. Trouabal, O. Roche, J.P. Jacquot, Analysis of light/dark synchronization of cell-wallless *Chlamydomonas reinhardtii* (Chlorophyta) cells by flow cytometry, Eur. J. Phycol. 34 (1999) 279–286.
[55] A. Garz, M. Sandmann, M. Rading, S. Ramm, R. Menzel, M. Steup, Cell-to-cell diversity in a synchronized Chlamydomonas culture as revealed by single-cell analyses, Biophys. J. 103 (2012) 1078–1086.
[56] K. Bisova, V. Zachleder, Cell-cycle regulation in green algae dividing by multiple fission, J. Exp. Bot. 65 (2014) 2585–2602.
[57] W.H.A. Ng, H. Liu, Diel variation of the cellular carbon to nitrogen ratio of Chlorella autotrophica (Chlorophyta) growing in phosphorous- and nitrogen-limited continuous cultures, J. Phycol. 51 (2015) 82–92.
[58] M. Siaut, S. Cuine, C. Cagnon, et al., Oil accumulation in the model green alga *Chlamydomonas reinhardtii*: characterization, variability between common laboratory strains and relationship with starch reserves, BMC Biotechnol. 11 (2011) Article Number: 7.
[59] M. Vitova, K. Bisova, D. Umysova, M. Hlavova, S. Kawano, V. Zachleder, M. Cizkova, *Chlamydomonas reinhardtii*: duration of its cell cycle and phases at growth rates affected by light intensity, Planta 233 (2011) 75–86.
[60] J. Coombs, P.J. Halicki, O. Holm Hansen, B.E. Volcani, Studies on biochemistry and fine structure of silica shell formation in diatoms: changes in concentration of nucleoside triphosphates during synchronized division of *Cylindrotheca fusiformis*, Exp. Cell Res. 47 (1967) 302–314.
[61] W.M. Darley, B.E. Volcani, Role of silicon in diatom metabolism: a silicon requirement for deoxyribonucleic acid synthesis in the diatom *Cylindrotheca fusiformis* Reimann and Lewin, Exp. Cell Res. 58 (1969) 334–342.

[62] S.W. Chisholm, F. Azam, R.W. Eppley, Silicic acid incorporation in marine diatoms on 1ight:dark cycles: use as an assay for phased cell division, Limnol. Oceanogr. 23 (1978) 518–529.
[63] R.W. Eppley, R.W. Holmes, E. Paasche, Periodicity in cell division and physiological behavior of *Ditylum brightwellii*, a marine planktonic diatom, during growth in light-dark cycles, Arch. Mikrobiol. 56 (1967) 305–323.
[64] T.C. Granata, Diel periodicity in growth and sinking rates of the centric diatom *Coscinodiscus concinnus*, Limnol. Oceanogr. 36 (1991) 132–139.
[65] X. Chen, K. Gao, Characterization of diurnal photosynthetic rhythms in the marine diatom *Skeletonema costatum* grown in synchronous culture under ambient and elevated CO_2, Funct. Plant Biol. 31 (2004) 399–404.
[66] J. Levering, J. Broddrick, C.L. Dupont, et al., Genome-scale model reveals metabolic basis of biomass partitioning in a model diatom, PLoS One 11 (2016), e0155038. .
[67] D.Y. Lee, O. Fiehn, High quality metabolomic data for *Chlamydomonas reinhardtii*, Plant Methods 4 (2008) Article Number: 7.